Effects of uphill and downhill walking on post-traumatic osteoarthritis development in mice

李, 昌欣

(Degree)
博士（保健学）

(Date of Degree)
2023-09-25

(Date of Publication)
2024-09-01

(Resource Type)
doctoral thesis

(Report Number)
甲第8735号

(URL)
https://hdl.handle.net/20.500.14094/0100485919

博　士　論　文

Effects of uphill and downhill walking on post-traumatic osteoarthritis development in mice

（マウスの外傷後変形性関節症に対する昇り坂および降り坂の歩行効果）

令和 5 年 6 月 25 日

神戸大学大学院保健学研究科保健学専攻

Changxin Li

李昌欣

Contents

Key points

Flat and uphill treadmill walking can prevent the development of post-traumatic osteoarthritis in mice.

Flat and uphill walking increases anabolic proteins and decreases catabolic proteins and inflammatory cytokines in articular cartilage, resulting in protection against cartilage degeneration.

Downhill walking increases catabolic proteins and inflammatory cytokines in cartilage, which has negative effects on articular cartilage.

Abstract

Using destabilization of the medial meniscus (DMM) induced models of osteoarthritis (OA), we sought to clarify how flat, uphill, and downhill walking affects OA-related inflammation and articular cartilage degeneration. Thirty-two male C57BL/6J mice of 7 weeks old underwent DMM surgery in their right knee and sham surgery in their left knee, and then were assigned to either the no walking after DMM group or the flat, uphill, or downhill walking after DMM group (n = 8/group). After creating the knee OA model, the mice in the walking groups were subjected to treadmill walking 1 day after

surgery, which included walking for 12 m/min, 30 min/day, and 7 days/week, with inclines of 0, 20, or − 20 degrees. Knee joints were harvested at the end of the intervention period. Non-demineralized frozen sections were prepared and samples were examined histologically. Osteoarthritis Research Society International scores were significantly decreased in both the uphill and flat walking groups, compared with the no-walking group. Immunohistochemical staining showed increased levels of aggrecan and Sry-related high mobility group box 9; conversely, decreased levels of Matrix metalloproteinase-13 and A disintegrin and metalloproteinase with thrombospondin motifs 5 in both the uphill and flat walking groups. Micro-CT results showed higher bone volume fraction in the uphill and flat walking groups than that in the no-walking group. Our findings indicate that flat and uphill walking may prevent the progression of OA.

Keywords

Osteoarthritis; Uphill walking; Downhill walking; Articular cartilage; Subchondral bone

Introduction

Osteoarthritis (OA) is characterized by articular cartilage degeneration, resulting in knee joint pain, dysfunction, and limitation of activities of daily living (Lawrence *et al.*, 2008; Bijlsma *et al.*, 2011). The incidence of OA is increasing due to the ageing population and the obesity epidemic. Currently, OA remains a challenge for clinicians and effective treatments are lacking. The definitive treatment for OA is total knee arthroplasty, which is associated with considerable burden and pain. Therefore, preventing the progression of OA is important for affected patients.

Physiological mechanical loading plays an important role in articular cartilage homeostasis. Physical exercise, a type of exogenous mechanical loading, is required for cartilage preservation (Eckstein *et al.*, 2006; Li *et al.*, 2011; Maly & Robbins, 2014; Iijima *et al.*, 2015; Blazek *et al.*, 2016; Oka *et al.*, 2021*a*, 2021*b*). In addition, exercise can prevent arthritic diseases in healthy cartilage by modulating extracellular matrix (ECM) biosynthesis/chondrogenesis and attenuating of inflammatory pathways. In animal OA models, moderate exercise suppresses articular cartilage degeneration, chondrocyte deaths, and pro-inflammatory cytokine levels (Galois *et al.*, 2004; Iijima *et al.*, 2015; Chen *et al.*, 2020). In addition, moderate-intensity exercise can inhibit the expression of Matrix metalloproteinases (MMPs), thereby reducing the excessive degradation of type II collagen and aggrecan by MMPs and A disintegrin and metalloproteinase with thrombospondin motifs (ADAMTS) (Kapoor *et al.*, 2011). Furthermore, moderate treadmill walking can be used to control joint pain and symptoms in patients with mild to

moderate knee OA (Peeler & Ripat, 2018), which may promote a more stable loading environment and reduce the risk of OA (Hafer *et al.*, 2019). On the contrary, excessive mechanical loading of the joints has negative effects on cartilage homeostasis. Excessive mechanical loading, such as in long-distance running (Beckett *et al.*, 2012) and high-impact sports (Sandmark & Vingård, 2007), damages the ECM, leading to cartilage deterioration and eventually OA (Sun, 2010). In addition, excessive exercise increases osteoclast activity and exacerbates OA disease (Franciozi *et al.*, 2013; Yamaguchi *et al.*, 2013; Morais *et al.*, 2021). Although high-intensity of exercise places excessive stress on cartilage, the inclination may also play a role in the strain on the knee. When comparing flat walking, a 54% increase in peak ground reaction force downhill and a 22% decrease uphill (Gottschall & Kram, 2005). Furthermore, uphill walking mainly elicits concentric contractions of the knee extensors and downhill elicits eccentric contractions, therefore the different contractile properties may affect the cartilage (Chavanelle *et al.*, 2014). Indeed, electrical stimulation-induced eccentric contractions of the rabbit quadriceps have been reported to result in greater knee loading than concentric contractions and cause chondrocyte death (Horisberger *et al.*, 2012). Thus, different inclinations may have different effects on the knee, but how walking at different inclinations affects OA development remains unclear.

Much of the previous research to date has focused on level walking. However, the etiology of OA development depends on the exercise conditions, especially the main type of muscle contraction and the load on the knee joint, which varies among flat, uphill, and downhill walking. The daily activities with OA patients include walking uphill and

downhill, as well as walking up and down stairs, in addition to flat walking. The relationship between different incline walking in OA under the same conditions has not been fully elucidated. Therefore, this study aimed to verify the effects of flat, uphill, and downhill walking on the development of OA. To reach our goal, we evaluated the effects of an incline treadmill walking on cartilage degeneration and subchondral bone changes following OA.

Materials and Methods

Ethical approval

All experimental procedures were approved by our institutional animal care and use committee and according to the Kobe University Animal Experimentation Regulations (approval number, P210617). The authors confirmed that this work complies with the Animal Research: Reporting of In Vivo Experiments (ARRIVE) checklist.

Animal care and surgical induction of osteoarthritis

In total, 32 male C57BL/6J mice, 7 weeks old, were purchased from Japan SLC (Shizuoka, Japan). After 1 week of acclimatization, all mice underwent the destabilization of the medial meniscus (DMM) surgery and were divided randomly into 4 groups: DMM, DMM + uphill, DMM + downhill, and DMM + flat groups (n = 8 mice per group). The DMM surgery was performed as previously described (Glasson *et al.*, 2007). Briefly, mice were anesthetized with isoflurane using NARCOBIT-EII type (Natsume Seisakusyo Inc.,

Tokyo, Japan). The surgery involved an incision into the medial capsule and transection of the anterior medial meniscotibial ligament (MMTL) on the right knee. A sham operation was performed on the left knee joint as an internal control using the same approach without transection of the MMTL. All surgical procedures were performed using the sterile technique with efforts made to minimize trauma to the animals. After surgery, mice received subcutaneous buprenorphine as an analgesic every 12 hours for 3 days. Animals were housed in polycarbonate cages with bedding (cedar shavings) and were maintained under artificial conditions at 22 ± 1°C, with a constant humidity of 55 ± 5%, and a 12-hours light/12-hours dark cycle. These animals had free access to standard food and water for 24 hours.

Treadmill walking exercise protocol

The exercise protocol of this study is shown in Figure 1. According to a previous study (Iijima *et al.*, 2015), 2-weeks of gentle treadmill walking began to show changes in biomechanical properties and superficial zone of the osteochondral region, and thereafter 4 weeks suppressed increasing osteocyte deaths and had a tendency to prevent osteoclasts generated in the DMM knee. Therefore, this study included a 1-week exercise adaptation and a 3-week intervention period to compare the differences between uphill and downhill walking exercises. Mice in the confined cage were randomly assigned into 4 groups consisting of the DMM group and 3 exercise groups (flat, uphill, and downhill groups). Mice in the DMM group were restricted to moving within the cage without additional exercise. The next day after DMM surgery, mice in the exercise groups were acclimated

to the treadmill environment for 7 days. Thereafter, the mice in the exercise groups were exercised on the treadmill (MK-680, Muromachi Kikai, Tokyo, Japan) at a constant speed of 12 m/min for 30 min/day, 7 days/week, set at 0, 20, and − 20 degrees of inclination, for 3 weeks. All animals survived throughout the experimental period and appeared to be healthy.

Micro-computed tomography

All animals were euthanized by exsanguination under general anesthesia and analgesia at the end of the experimental period. The distal femur and proximal tibia were scanned with a micro-three-dimensional X-ray CT system (R_mCT2; Rigaku, Tokyo, Japan) with an isotropic voxel resolution of 20 μm, operating at a voltage of 90 kV, current of 160 μA, and a scan time of 3 min per sample. The 3D images were reconstructed. After 3D reconstruction, the region of interest (ROI: 500 μm × 800 μm × 400 μm) for bone microarchitecture measurements was manually selected to cover most of the subchondral bone of the medial tibial plateau, which is the most affected by DMM surgery (Das Neves Borges *et al.*, 2014). Bone mineral density (BMD) and bone volume fraction (BV/TV) within the ROI were quantitatively analyzed using TRI/3D-BON software (Ratoc, Tokyo, Japan) according to the μCT analysis guidelines (Bouxsein *et al.*, 2010). Briefly, trabecular and cortical bone were automatically separated using the software with thresholds of 599 mg HA/cm^3, and calculation of BMD and BV/TV.

Histology

Histological preparation

After μCT analysis, undecalcified frozen sections were prepared according to the method described by Kawamoto (Kawamoto, 2003). Briefly, the whole knee joints including the patella and joint capsule were freeze-embedded in a super cryo-embedding medium (SCEM, Leica Microsystems, Tokyo, Japan) in isopentane at − 75°C. Cross-sections of the knee joints in the coronal plane (5 μm thick) were cut from each sample and used for histological or immunohistochemical analyses.

Histomorphometric analysis

As we have reported previously (Moriyama *et al.*, 2008; Nomura *et al.*, 2017), the medial tibial plateaus were defined as the regions of the articular cartilage evaluation area. Articular cartilage thickness and chondrocyte density were measured from digitized images of hematoxylin and eosin-stained histological sections. Briefly, a 400 μm long stretch of the cartilage surface was defined for each region, and the areas of the uncalcified and calcified cartilage under this stretch were measured separately. The thickness of each layer was calculated by dividing the area by 400 μm. Total cartilage thickness was the sum of the thickness of the uncalcified and calcified layers. Chondrocyte density was determined as the number of chondrocytes per cartilage area. Cartilage damage was graded according to the Osteoarthritis Research Society International (OARSI) guidelines (Glasson *et al.*, 2010). Three blinded graders (C.L., S.I., and J.H.) scored 2 regions (medial tibial plateaus and medial femoral condyles) of the knee from 8 mice per group. A score of 0 = normal cartilage, 0.5 = loss of proteoglycan

with an intact surface, 1 = superficial fibrillation without loss of cartilage, 2 = vertical clefts and loss of surface lamina (any % or joint surface area), 3 = vertical clefts/erosion to the calcified layer lesion for 1-25% of the quadrant width, 4 = lesion reaches the calcified cartilage for 25-50% of the quadrant width, 5 = lesion reaches the calcified cartilage for 50-75% of the quadrant width, 6 = lesion reaches the calcified cartilage for > 75% of the quadrant width. The total OARSI scores reflect the sum of the 2 regional scores. Cartilage proteoglycan content was assessed in the histological sections to quantify the Safranin O staining intensity as previously described (Griffin *et al.*, 2012). Briefly, histological images were converted to grayscale images with Adobe Photoshop CS2 (Adobe Systems, San Jose, CA, USA), and the mean of pixel gray values in the articular cartilage, growth plate, and subchondral bone was measured with ImageJ (1.50b; National Institutes of Health, Bethesda, MD, USA). To allow comparison between each section, the pixel value of the growth plate and the subchondral bone were used for calibration as the sites with maximal and minimal proteoglycan content, respectively. Safranin O staining intensity was calculated by the following formula: Staining intensity = $100 \times \{(I_{sb} - I_c)/(I_{sb} - I_{gp})]$, where I is the mean pixel value of the subchondral bone (I_{sb}), articular cartilage (I_c), and growth plate (I_{gp}).

Immunohistochemical analysis

According to the protocols established in our laboratory (Moriyama *et al.*, 2012), the frozen sections were incubated with anti-SRY-related high-mobility-group box 9 (Sox9) (diluted 1:500, ab3639, Abcam, Cambridge, UK), anti-type II collagen (diluted 1:200,

ab21291, Abcam), anti-aggrecan (diluted 1:400, AB1031, Chemicon, Tokyo, Japan), anti-MMP-13 (diluted 1:400, ab39012, Abcam), and anti-ADAMTS5 (diluted 1:500, ab41037, Abcam), anti-Interleukin-6 (IL-6) (diluted 1:200, AB6672, Abcam), and anti-Tumor necrosis factor-α (TNF-α) (diluted 1:100, ab6671, Abcam), antibodies. A subsequent reaction was made using the streptavidin-biotin-peroxidase complex technique with an Elite ABC kit (diluted 1: 50, PK-610, Vector Laboratories, Burlingame, USA). ImmPACT DAB (SK-4105, Vector Laboratories) was then used for visualizing the immunoreaction. Finally, the sections were counterstained with Dako Real Hematoxylin, washed in water, and mounted. The immunolabeled sections were captured with a light microscope (BX53; Olympus, Tokyo, Japan) and camera (DP73; Olympus, Tokyo, Japan) at 4× or 20× magnification in the central 400 μm × 200 μm area of the medial tibial plateau. Type II collagen staining intensity was calculated by measuring pixel values of articular cartilage, growth cartilage, and subchondral bone using ImageJ, as well as Safranin O staining intensity. For MMP-13, ADAMTS5, Sox9, aggrecan, TNF-α, and IL-6, the number of immune-positive cells were counted manually, and the positive cell density was calculated by dividing the number of positive cells by the area.

Statistical analysis

Statistical analyses were conducted with EZR (Saitama Medical Center, Jichi Medical University, Saitama, Japan), which is a graphical user interface for R (The R Foundation for Statistical Computing, Vienna, Austria) (Kanda, 2013). First, the Shapiro-Wilk test was used to check the normality of the distribution for each data set. The OARSI score

was compared between groups using the Kruskal-Wallis test with a Steel-Dwass post hoc analysis. The histomorphologic and immunohistochemical results were compared among groups using analysis of variance with Tukey's post hoc test. Parametric data are shown as the mean ± standard deviation (SD), whereas nonparametric data are shown as the median with interquartile range. All significance thresholds were set at 5%.

Results

Subchondral bone changes after treadmill walking

The 3D reconstruction of knee joints from micro-CT analyses is shown in Figure 2A. As seen in the coronal plane images, irregular bone surface and abnormal patellar shape (osteophyte formation) were not observed in DMM mice at 4 weeks post-surgery (Fig. 2A). Bone sclerosis was observed in the medial tibial plateau at 4 weeks after DMM compared to the sham joint (Figure 2A, white arrows). BMD in the exercise groups showed no statistical differences when compared with the DMM group at 4 weeks post-surgery (Fig. 2B). The knee joints that received DMM surgery had higher BV/TV than their sham knee joints. Flat (P = 0.0342) and uphill (P = 0.0271) treadmill walking significantly increased BV/TV in the medial tibial plateau compared to the DMM group (Fig. 2C).

Cartilage changes after treadmill walking

The OA phenotype after DMM surgery was confirmed by histology with Safranin-O/Fast

Green staining (Fig. 3A). Osteophyte formation or synovial abnormalities were not observed in all groups. However, proteoglycan loss, fissure, fibrillation, the surface undulation of the upper zone of the articular cartilage, and mild to moderate cartilage damage were present on the medial tibial plateau in the surgical joints of DMM mice (Fig. 3A, white arrows). In the medial compartments of the joint, OARSI scores were higher in the DMM ($P = 0.0030$), DMM + flat ($P = 0.0029$), DMM + uphill ($P = 0.0030$), and DMM + downhill ($P = 0.0031$) groups than that of the sham groups (Fig. 3B). The scores in the DMM + flat ($P = 0.0158$) and DMM + uphill ($P = 0.0480$) groups significantly decreased compared to the DMM group (Fig. 3B). The analyzed interobserver reliability of OARSI scoring was ICC (1,1) = 0.803 and 95% CI = ($0.695 < ICC < 0.882$). Safranin-O staining intensity showed no differences between the DMM group and each exercise group (Fig. 3C).

Cartilage thickness and chondrocyte density

Cartilage thickness and chondrocyte density in the uncalcified, calcified, and total layer did not change among the groups (Fig. 4).

Cartilage anabolic and catabolic proteins change after treadmill walking

As shown by immunohistochemistry, type II collagen was evenly distributed throughout the cartilage (Fig. 5A), and the staining intensity did not differ among the groups (Fig. 5B). There was evidence of a relative increase in aggrecan-positive chondrocytes in the DMM + uphill group compared to the DMM group ($P = 0.0700$) (Fig. 5C). Aggrecan-

positive chondrocytes increased in both the uncalcified (P = 0.0065) and total (P = 0.0035) layers of cartilage in the DMM + uphill group, when compared with the DMM + flat group (Fig. 5C). Sox9 positive chondrocytes increased in the DMM + uphill group in the uncalcified ($P < 0.0001$), calcified ($P = 0.0005$), and total ($P < 0.0001$) layers relative to the DMM group (Fig. 5D). Sox9-positive chondrocytes increased in the DMM + uphill group in the uncalcified ($P < 0.0001$) and total ($P < 0.0001$) layers, when compared with the DMM + flat group (Fig. 5D). The DMM + downhill group was also up-regulated in the calcified ($P = 0.0281$) and total ($P = 0.0253$) layers relative to the DMM group (Fig. 5D). Sox9-positive chondrocytes decreased in the uncalcified ($P = 0.0006$) and total ($P <$ 0.0001) layers of cartilage in the DMM + downhill group relative to the DMM + uphill group (Fig. 5D).

There was a decrease in MMP-13-positive chondrocytes in the calcified (P = 0.0030) and total ($P = 0.0218$) layers in the DMM + uphill group compared to the DMM group (Fig. 6B). ADAMTS5-positive chondrocytes in the DMM + flat, DMM + uphill and DMM + downhill groups in the uncalcified ($P = 0.0003$, $P < 0.0001$ and $P = 0.0010$, respectively) and total (P = 0.0001, $P < 0.0001$ and $P = 0.0044$, respectively) cartilage significantly decreased in comparison with the DMM group (Fig. 6C).

Cartilage inflammatory proteins change after treadmill walking

IL-6- and TNF-α-positive chondrocytes decreased in both the uncalcified ($P = 0.0002$ and $P = 0.0005$, respectively) and total ($P = 0.0002$ and $P = 0.0105$, respectively) layers

of cartilage in the DMM + uphill group relative to the DMM group (Fig. 7B and C). Positive chondrocytes for IL-6 in the DMM + downhill group ($P = 0.0284$) and for TNF-α in the DMM + flat group ($P = 0.0239$) were decreased in the uncalcified layer compared with the DMM group (Fig. 7B and C). In addition, IL-6-positive chondrocytes decreased in the total layer cartilage in the DMM +uphill group relative to the DMM + flat group ($P = 0.0436$) (Fig. 7B). TNF-α positive chondrocytes increased in the uncalcified layer cartilage in the DMM + downhill group relative to the DMM + uphill group ($P = 0.0225$) (Fig. 7C).

Discussion

In the present study, the effects of uphill, downhill, and flat walking were evaluated in a mouse model of post-traumatic OA. Our results showed that flat and uphill walking increase bone remodeling occurring in the early stages of OA. We also observed decreased OARSI scores in the uphill and flat walking groups. In addition, uphill walking increased the levels of cartilage anabolic proteins and decreased the levels of catabolic proteins and inflammatory cytokines. These results suggest that flat and uphill walking prevented the progression of both articular cartilage and subchondral bone lesions during OA development, indicating the beneficial role of moderate flat and uphill walking

training in the DMM model of OA.

Remodeling of subchondral bone has been implicated as one of the major factors involving in cartilage degeneration. Articular cartilage may play an essential role in regulating the mechanical loading of subchondral bone (Carlson *et al.*, 1996; Suri & Walsh, 2012; Shen *et al.*, 2013; Zhen *et al.*, 2013). Furthermore, impaired biomechanical integrity of cartilage could induce abnormal bone remodeling in an attempt to repair bone microdamage (Seref-Ferlengez *et al.*, 2015; McCann *et al.*, 2017). However, how uphill or downhill walking affects subchondral bone changes remains unclear. Consistent with a previous study (Fang *et al.*, 2018), DMM surgery induced subchondral bone sclerosis in the medial tibial plateau. In addition, flat and uphill walking further increased its subchondral bone volume, but downhill walking did not. Some reports have shown that flat walking increases subchondral bone volume in DMM rats (Iijima *et al.*, 2015; Hao *et al.*, 2022). Although the increase in subchondral bone leads to the disruption of subchondral bone homeostasis (Goldring & Goldring, 2010), a previous report (Iijima *et al.*, 2015) suggests that the increase in subchondral bone after flat walking is associated with the prevention of subchondral bone cysts and cartilage degeneration. Besides flat walking, our results show that uphill walking may also prevent subchondral bone deterioration and fragility. Additionally, the histological results by the OARSI scoring system showed that the DMM + flat and DMM + uphill groups had less cartilage destruction and their OARSI scores also decreased. This result is congruent with a previous report (Morais *et al.*, 2021), suggesting that uphill and flat treadmill walking inhibit osteocyte deaths induced by DMM surgery and positively correlate with OARSI

scores. Taken together, this study confirmed that moderate flat and uphill walking interventions can improve subchondral bone remodeling, bone strength, and weight-bearing capacity in OA. In addition, uphill and flat walking has possibilities for the future in protecting cartilage degeneration following OA.

Cartilage homeostasis, a phase in which ECM synthesis is balanced by degradation, is critical for joint health (Mobasheri *et al.*, 2017). The progression of OA is associated with changes in the cartilage ECM network formed by type II collagen and aggrecan matrix proteins (Goldring & Marcu, 2009). In addition, ECM synthesis is regulated by transcriptional regulators involved in chondrogenesis, specifically, Sox9, which regulates type II collagen and aggrecan gene expression (Yeung Tsang *et al.*, 2014). Our results showed increased expression of the chondrogenic markers, aggrecan, and Sox9, in the DMM + uphill group. In support of these, some previous studies (Song & Park, 2020; Haseeb *et al.*, 2021) suggest that uphill treadmill walking maintains a durable cartilage matrix through Sox9 upregulation and directs the rescue response of chondrocytes to trauma. Together with the results of the previous results, our findings provide strong evidence that uphill waking has a protective effect on the articular cartilage in mice with OA induced by DMM surgery. On the other hand, catabolic events are dominant in OA, and cells are exposed to degenerative enzymes such as aggrecanases (ADAMTS5) and collagenases (MMP-13), which have implications for articular cartilage degeneration (Yoon *et al.*, 2000; Parks *et al.*, 2004; Gilbert *et al.*, 2011). Meanwhile, in the ECM of OA cartilage, MMP-13 is the major degrading enzyme for collagen, and ADAMTS5 is the major degrading proteinase for aggrecan (Jung *et al.*, 2019; Feng *et al.*,

2020). Taken together, our results showed that flat and uphill walking suppresses the cartilage degenerating enzymes, resulting in attenuation of OA.

During the progression of OA, inflammatory cytokines, the most important compounds in the pathogenesis of OA, have the greatest influence on anabolic and catabolic processes (Wojdasiewicz *et al.*, 2014). TNF-α and IL-6 mediate the activation of MMPs in the ECM of the articular cartilage, leading to cartilage destruction (Maldonado & Nam, 2013; Malemud, 2015). In addition, TNF-α increases the inflammation and catabolism in joint tissues (Roman-Blas & Jimenez, 2006) and plays a role in blocking the synthesis of collagen and proteoglycan in chondrocytes (Saklatvala, 1986; Séguin & Bernier, 2003). IL-6 inhibits type II collagen production and upregulates MMP-13 and ADAMTS5 gene expression in chondrocytes (Cawston *et al.*, 1998; Rowan *et al.*, 2001; Porée *et al.*, 2008). A previous report (Nam *et al.*, 2011) has demonstrated a direct anti-inflammatory effect of moderate treadmill walking on knee OA. Moderate treadmill walking can alleviate the severity of cartilage lesions in experimental OA through its anti-inflammatory capacity (Galois *et al.*, 2004; Na *et al.*, 2014). In this study, our data showed that uphill/flat treadmill walking reduced the expressions of TNF-α and IL-6 in the OA cartilage, indicating a reduction in cartilage damage.

Articular cartilage lesions and osteophytes in OA are present in the medial tibial plateau of the DMM knees in the first 2 weeks and become progressively more severe by 16 weeks (Loeser *et al.*, 2013). The early phase at 2 and 4 weeks after DMM surgery was the most active in terms of gene expression (Loeser *et al.*, 2013), highlighting the importance of the timing of the intervention for OA treatment. Gentle treadmill

walking for 4 weeks also tended to suppress the growth of osteoclasts and osteocyte deaths (Iijima *et al.*, 2015). In line with our findings, exercise intervention at the early phase of cartilage damage provided greater benefits in monoiodoacetate-induced OA (Nam *et al.*, 2009). Our results also confirm the efficacy of the early (4 weeks) treadmill walking in preventing the development of OA.

Notably, in the present study, uphill walking improved OA, but not when downhill walking, which is consistent with a previous study (Morais *et al.*, 2021). The mechanical load on the knee is greater during downhill walking than during uphill walking exercises (Gottschall & Kram, 2005; Horisberger *et al.*, 2012). This is because eccentric exercise, such as downhill walking, may cause more damage and increase pro-inflammatory insult than concentric exercise (uphill walking) (Heinlein *et al.*, 2009; Horisberger *et al.*, 2012). Eccentric exercise induces muscle damage and cartilage and bone degeneration. (Horisberger *et al.*, 2012). Excessive mechanical stress on cartilage leads to inflammation (Morais *et al.*, 2021). Indeed, in the present study, TNF-α was higher during downhill walking than during uphill walking. Therefore, downhill walking may result in excessive stress on the knee, and consequently, cause an increase in TNF-α and catabolic proteins (MMP-13) promoting OA cartilage damage.

This study has several potential limitations. First, the study was conducted at only one time point (i.e., 4 weeks after DMM) that only includes the early stages of OA. Iijima *et al*. (2015) have reported that flat walking for at least 4 weeks after DMM, rather than 1 or 2 weeks, resulted in a chondroprotective effect. In our study, the chondroprotective effect of walking was also observed at 4 weeks after DMM, and this

time point was sufficient to reveal the effects of walking on OA. However, we could not determine the effect of treadmill walking in the late stages of OA. Further studies including the effects of long-term treadmill walking on cartilage and subchondral bone are warranted. Second, we used an experimental mouse OA model by DMM-induced injury, much more severe than the joint degeneration observed in humans. This is a common limitation of all mouse OA models involving knee instability. Therefore, our results may not be directly applicable to humans. Finally, the lack of diversity in the exercise protocol. Although our exercise protocol was consistent with previous studies that evaluated chondroprotective in the knee joint in instability-induced OA mouse models (12-30 m/min for 30-60 min/day, 3-7 days/week) (Pate *et al.*, 2015; Oka *et al.*, 2021*a*, 2021*b*; Zhou *et al.*, 2021). Since articular cartilage responds to mechanical stimuli in a dose-dependent manner (Nam *et al.*, 2009, 2011; Ni *et al.*, 2012), it would be worthwhile to elucidate the effects on cartilage and subchondral bone under different protocols.

In conclusion, our findings demonstrated the beneficial role of early flat and uphill walking in preventing the progression of OA. The potential mechanism is that flat and uphill walking attenuates the structural and functional OA progression by inhibiting the expression of MMP-13, ADAMTS5, TNF-α, and IL-6. In addition, this study suggests that downhill walking does not have beneficial results and may not be an effective strategy for the treatment of OA.

Additional information

Data availability statement

The datasets used and analyzed during this study are available from the corresponding author upon request.

Competing interests

The authors have no conflicts of interest.

Author contributions

CL was responsible for conducting the experiment, extracting and analyzing data, interpreting results, and writing the manuscript. HM and OS were responsible for designing and directing the protocol, interpreting results, and revising the manuscript. SI, JH, HJ, and DT were responsible for conducting the experiment, extracting and analyzing data, and revising the manuscript. All authors have approved the final submitted manuscript.

Funding

Two of the authors (HM and CL) has received funding from the Japan Society for the Promotion of Science (JSPS) KAKENHI Grant No. 19H04050 and Japan Science and Technology Agency (Support for Pioneering Research Initiated by the Next Generation).

Acknowledgments

We thank Masato Nomura, Yoshio Wakimoto and Toshikazu Ito for their skilled technical assistance. Each author certifies that he has no commercial associations (eg, consultancies, stock ownership, equity interest, patent/licensing arrangements, etc) that might pose a conflict of interest in connection with the submitted article. Each author certifies that his institution approved the animal protocol for this investigation and that all investigations were conducted in conformity with ethical principles of research.

References

1. Beckett J, Jin W, Schultz M, Chen A, Tolbert D, Moed BR & Zhang Z (2012). Excessive running induces cartilage degeneration in knee joints and alters gait of rats. *Journal of Orthopaedic Research* **30,** 1604–1610.
2. Bijlsma JWJ, Berenbaum F & Lafeber FPJG (2011). Osteoarthritis: An update with relevance for clinical practice. *The Lancet* **377,** 2115–2126.
3. Blazek AD, Nam J, Gupta R, Pradhan M, Perera P, Weisleder NL, Hewett TE, Chaudhari AM, Lee BS, Leblebicioglu B, Butterfield TA & Agarwal S (2016). Exercise-driven metabolic pathways in healthy cartilage. *Osteoarthritis Cartilage* **24,** 1210–1222.
4. Bouxsein ML, Boyd SK, Christiansen BA, Guldberg RE, Jepsen KJ & Müller R (2010). Guidelines for assessment of bone microstructure in rodents using micro-computed tomography. *Journal of Bone and Mineral Research* **25,** 1468–1486.

5. Carlson CS, Loeser RF, Purser CB, Gardin JF & Jerome CP (1996). Osteoarthritis in cynomolgus macaques III: Effects of age, gender, and subchondral bone thickness on the severity of disease. *Journal of Bone and Mineral Research* **11,** 1209–1217.
6. Cawston TE, Curry VA, Summers CA, Clark IM, Riley GP, Life PF, Spaull JR, Goldring MB, Koshy PJT, Rowan AD & Shingleton WD (1998). The role of oncostatin M in animal and human connective tissue collagen turnover and its localization within the rheumatoid joint. *Arthritis Rheum* **41,** 1760–1771.
7. Chavanelle V, Sirvent P, Ennequin G, Caillaud K, Montaurier C, Morio B, Boisseau N & Richard R (2014). Comparison of oxygen consumption in rats during uphill (concentric) and downhill (eccentric) treadmill exercise tests. *J Sports Sci Med* **13,** 689–694.
8. Chen L, Lou Y, Pan Z, Cao X, Zhang L, Zhu C & Liang J (2020). Treadmill and wheel exercise protect against JNK/NF-κB induced inflammation in experimental models of knee osteoarthritis. *Biochem Biophys Res Commun* **523,** 117–122.
9. Eckstein F, Hudelmaier M & Putz R (2006). The effects of exercise on human articular cartilage. *J Anat* **208,** 491–512.
10. Fang H, Huang L, Welch I, Norley C, Holdsworth DW, Beier F & Cai D (2018). Early Changes of Articular Cartilage and Subchondral Bone in The DMM Mouse Model of Osteoarthritis. *Sci Rep* **8,** 2855.
11. Feng X, Pan J, Li J, Zeng C, Qi W, Shao Y, Liu X, Liu L, Xiao G, Zhang H, Bai X & Cai D (2020). Metformin attenuates cartilage degeneration in an

experimental osteoarthritis model by regulating AMPK/mTOR. *Aging* **12,** 1087–1103.

12. Franciozi CES, Tarini VAF, Reginato RD, Gonçalves PRS, Medeiros VP, Ferretti M, Dreyfuss JL, Nader HB & Faloppa F (2013). Gradual strenuous running regimen predisposes to osteoarthritis due to cartilage cell death and altered levels of glycosaminoglycans. *Osteoarthritis Cartilage* **21,** 965–972.
13. Galois L, Etienne S, Grossin L, Watrin-Pinzano A, Cournil-Henrionnet C, Loeuille D, Netter P, Mainard D & Gillet P (2004). Dose-response relationship for exercise on severity of experimental osteoarthritis in rats: A pilot study. *Osteoarthritis Cartilage* **12,** 779–786.
14. Gilbert AM, Bikker JA & O'Neil S V. (2011). Advances in the development of novel aggrecanase inhibitors. *Expert Opin Ther Pat* **21,** 1–12.
15. Glasson SS, Blanchet TJ & Morris EA (2007). The surgical destabilization of the medial meniscus (DMM) model of osteoarthritis in the 129/SvEv mouse. *Osteoarthritis Cartilage* **15,** 1061–1069.
16. Glasson SS, Chambers MG, Van Den Berg WB & Little CB (2010). The OARSI histopathology initiative - recommendations for histological assessments of osteoarthritis in the mouse. *Osteoarthritis Cartilage* **18,** S18–S23.
17. Goldring MB & Goldring SR (2010). Articular cartilage and subchondral bone in the pathogenesis of osteoarthritis. *Ann N Y Acad Sci* **1192,** 230–237.
18. Goldring MB & Marcu KB (2009). Cartilage homeostasis in health and rheumatic diseases. *Arthritis Res Ther* **11,** 224.

19. Gottschall JS & Kram R (2005). Ground reaction forces during downhill and uphill running. *J Biomech* **38,** 445–452.
20. Griffin TM, Huebner JL, Kraus VB, Yan Z & Guilak F (2012). Induction of osteoarthritis and metabolic inflammation by a very high-fat diet in mice: Effects of short-term exercise. *Arthritis Rheum* **64,** 443–453.
21. Hafer JF, Kent JA & Boyer KA (2019). Physical activity and age-related biomechanical risk factors for knee osteoarthritis. *Gait Posture* **70,** 24–29.
22. Hao X, Zhang J, Shang X, Sun K, Zhou J, Liu J, Chi R & Xu T (2022). Exercise modifies the disease-relevant gut microbial shifts in post-traumatic osteoarthritis rats. *Bone Joint Res* **11,** 214–225.
23. Haseeb A, Kc R, Angelozzi M, de Charleroy C, Rux D, Tower RJ, Yao L, da Silva RP, Pacifici M, Qin L & Lefebvre V (2021). SOX9 keeps growth plates and articular cartilage healthy by inhibiting chondrocyte dedifferentiation/ osteoblastic redifferentiation. *Proc Natl Acad Sci U S A* **118,** 1–11.
24. Heinlein B, Kutzner I, Graichen F, Bender A, Rohlmann A, Halder AM, Beier A & Bergmann G (2009). ESB clinical biomechanics award 2008: Complete data of total knee replacement loading for level walking and stair climbing measured in vivo with a follow-up of 6-10 months. *Clinical Biomechanics* **24,** 315–326.
25. Horisberger M, Fortuna R, Leonard TR, Valderrabano V & Herzog W (2012). The influence of cyclic concentric and eccentric submaximal muscle loading on cell viability in the rabbit knee joint. *Clinical Biomechanics* **27,** 292–298.
26. Iijima H, Aoyama T, Ito A, Yamaguchi S, Nagai M, Tajino J, Zhang X & Kuroki

H (2015). Effects of short-term gentle treadmill walking on subchondral bone in a rat model of instability-induced osteoarthritis. *Osteoarthritis Cartilage* **23,** 1563–1574.

27. Jung YK, Park HR, Cho HJ, Jang JA, Lee EJ, Han MS, Kim GW & Han S (2019). Degrading products of chondroitin sulfate can induce hypertrophy-like changes and MMP-13/ADAMTS5 production in chondrocytes. *Sci Rep* **9,** 1–11.
28. Kanda Y (2013). Investigation of the freely available easy-to-use software "EZR" for medical statistics. *Bone Marrow Transplant* **48,** 452–458.
29. Kapoor M, Martel-Pelletier J, Lajeunesse D, Pelletier JP & Fahmi H (2011). Role of proinflammatory cytokines in the pathophysiology of osteoarthritis. *Nat Rev Rheumatol* **7,** 33–42.
30. Kawamoto T (2003). Use of a new adhesive film for the preparation of multi-purpose fresh-frozen sections from hard tissues, whole-animals, insects and plants. *Arch Histol Cytol* **66,** 123–143.
31. Lawrence RC, Felson DT, Helmick CG, Arnold LM, Choi H, Deyo RA, Gabriel S, Hirsch R, Hochberg MC, Hunder GG, Jordan JM, Katz JN, Kremers HM & Wolfe F (2008). Estimates of the prevalence of arthritis and other rheumatic conditions in the United States. Part II. *Arthritis Rheum* **58,** 26–35.
32. Li J, Anemaet W, Diaz MA, Buchanan S, Tortorella M, Malfait AM, Mikecz K, Sandy JD & Plaas A (2011). Knockout of ADAMTS5 does not eliminate cartilage aggrecanase activity but abrogates joint fibrosis and promotes cartilage aggrecan deposition in murine osteoarthritis models. *Journal of Orthopaedic Research* **29,**

516–522.

33. Loeser RF, Olex AL, McNulty MA, Carlson CS, Callahan M, Ferguson C & Fetrow JS (2013). Disease progression and phasic changes in gene expression in a mouse model of osteoarthritis. *PLoS One* **8,** e54633.
34. Maldonado M & Nam J (2013). The role of changes in extracellular matrix of cartilage in the presence of inflammation on the pathology of osteoarthritis. *Biomed Res Int* **2013,** 284873.
35. Malemud CJ (2015). Biologic basis of osteoarthritis: State of the evidence. *Curr Opin Rheumatol* **27,** 289–294.
36. Maly MR & Robbins SM (2014). Osteoarthritis year in review 2014: Rehabilitation and outcomes. *Osteoarthritis Cartilage* **22,** 1958–1988.
37. McCann MR, Yeung C, Pest MA, Ratneswaran A, Pollmann SI, Holdsworth DW, Beier F, Dixon SJ & Séguin CA (2017). Whole-body vibration of mice induces articular cartilage degeneration with minimal changes in subchondral bone. *Osteoarthritis Cartilage* **25,** 770–778.
38. Mobasheri A, Rayman MP, Gualillo O, Sellam J, Van Der Kraan P & Fearon U (2017). The role of metabolism in the pathogenesis of osteoarthritis. *Nat Rev Rheumatol* **13,** 302–311.
39. Morais GP, Chemerka C, Masson A, Seerattan R-A, da Rocha AL, Krawetz R, da Silva ASR & Herzog W (2021). Excessive downhill training leads to early onset of knee osteoarthritis. *Osteoarthritis Cartilage* **29,** 870–881.
40. Moriyama H, Kanemura N, Brouns I, Pintelon I, Adriaensen D, Timmermans JP,

Ozawa J, Kito N, Gomi T & Deie M (2012). Effects of aging and exercise training on the histological and mechanical properties of articular structures in knee joints of male rat. *Biogerontology* **13,** 369–381.

41. Moriyama H, Yoshimura O, Kawamata S, Takayanagi K, Kurose T, Kubota A, Hosoda M & Tobimatsu Y (2008). Alteration in articular cartilage of rat knee joints after spinal cord injury. *Osteoarthritis Cartilage* **16,** 392–398.
42. Na SS, Kim SG, Yong MS & Hwangbo G (2014). Study of Treadmill Exercise Effect on Rats with Osteoarthritis Using Proteomic Analysis. *Journal Physical Therapy Science* **26,** 487–490.
43. Nam J, Aguda BD, Rath B & Agarwal S (2009). Biomechanical thresholds regulate inflammation through the NF-kappaB pathway: experiments and modeling. *PLoS One* **4,** e5262.
44. Nam J, Perera P, Liu J, Wu LC, Rath B, Butterfield TA & Agarwal S (2011). Transcriptome-wide gene regulation by gentle treadmill walking during the progression of monoiodoacetate-induced arthritis. *Arthritis Rheum* **63,** 1613–1625.
45. Das Neves Borges P, Forte AE, Vincent TL, Dini D & Marenzana M (2014). Rapid, automated imaging of mouse articular cartilage by microCT for early detection of osteoarthritis and finite element modelling of joint mechanics. *Osteoarthritis Cartilage* **22,** 1419–1428.
46. Ni G-X, Lei L & Zhou Y-Z (2012). Intensity-dependent effect of treadmill running on lubricin metabolism of rat articular cartilage. *Arthritis Res Ther* **14,** R256.

47. Nomura M, Sakitani N, Iwasawa H, Kohara Y, Takano S, Wakimoto Y, Kuroki H & Moriyama H (2017). Thinning of articular cartilage after joint unloading or immobilization. An experimental investigation of the pathogenesis in mice. *Osteoarthritis Cartilage* **25,** 727–736.

48. Oka Y, Murata K, Kano T, Ozone K, Arakawa K, Kokubun T & Kanemura N (2021*a*). Impact of Controlling Abnormal Joint Movement on the Effectiveness of Subsequent Exercise Intervention in Mouse Models of Early Knee Osteoarthritis. *Cartilage* **13,** 1334S-1344S.

49. Oka Y, Murata K, Ozone K, Kano T, Minegishi Y, Kuro-Nakajima A, Arakawa K, Kokubun T & Kanemura N (2021*b*). Treadmill exercise after controlled abnormal joint movement inhibits cartilage degeneration and synovitis. *Life* **11,** 1–13.

50. Parks WC, Wilson CL & López-Boado YS (2004). Matrix metalloproteinases as modulators of inflammation and innate immunity. *Nat Rev Immunol* **4,** 617–629.

51. Pate KM, Sherk VD, Dana Carpenter R, Weaver M, Crapo S, Gally F, Chatham LS, Goldstrohm DA, Crapo JD, Kohrt WM, Bowler RP, Oberley-Deegan RE & Regan EA (2015). The beneficial effects of exercise on cartilage are lost in mice with reduced levels of ECSOD in tissues. *J Appl Physiol* **118,** 760–767.

52. Peeler J & Ripat J (2018). The effect of low-load exercise on joint pain, function, and activities of daily living in patients with knee osteoarthritis. *Knee* **25,** 135–145.

53. Porée B, Kypriotou M, Chadjichristos C, Beauchef G, Renard E, Legendre F, Melin M, Gueret S, Hartmann DJ, Malléin-Gerin F, Pujol JP, Boumediene K &

Galéra P (2008). Interleukin-6 (IL-6) and/or soluble IL-6 receptor down-regulation of human type II collagen gene expression in articular chondrocytes requires a decrease of Sp1·Sp3 ratio and of the binding activity of both factors to the COL2A1 promoter. *Journal of Biological Chemistry* **283,** 4850–4865.

54. Roman-Blas JA & Jimenez SA (2006). NF-κB as a potential therapeutic target in osteoarthritis and rheumatoid arthritis. *Osteoarthritis Cartilage* **14,** 839–848.
55. Rowan AD, Koshy PJT, Shingleton WD, Degnan BA, Heath JK, Vernallis AB, Spaull JR, Life PF, Hudson K & Cawston TE (2001). Synergistic effects of glycoprotein 130 binding cytokines in combination with interleukin-1 on cartilage collagen breakdown. *Arthritis Rheum* **44,** 1620–1632.
56. Saklatvala J (1986). Tumour necrosis factor alpha stimulates resorption and inhibits synthesis of proteoglycan in cartilage. *J Natl Med Assoc* **90,** 547–549.
57. Sandmark H & Vingård E (2007). Sports and risk for severe osteoarthrosis of the knee. *Scand J Med Sci Sports* **9,** 279–284.
58. Séguin CA & Bernier SM (2003). TNFα Suppresses Link Protein and Type II Collagen Expression in Chondrocytes: Role of MEK1/2 and NF-κB Signaling Pathways. *J Cell Physiol* **197,** 356–369.
59. Seref-Ferlengez Z, Kennedy OD & Schaffler MB (2015). Bone microdamage, remodeling and bone fragility: how much damage is too much damage? *Bonekey Rep* **4,** 1–7.
60. Shen J, Li J, Wang B, Jin H, Wang M, Zhang Y, Yang Y, Im HJ, O'Keefe R & Chen D (2013). Deletion of the transforming growth factor β Receptor type II

gene in articular chondrocytes leads to a progressive osteoarthritis-like phenotype in mice. *Arthritis Rheum* **65,** 3107–3119.

61. Song H & Park KH (2020). Regulation and function of SOX9 during cartilage development and regeneration. *Semin Cancer Biol* **67,** 12–23.
62. Sun HB (2010). Mechanical loading, cartilage degradation, and arthritis. *Ann N Y Acad Sci* **1211,** 37–50.
63. Suri S & Walsh DA (2012). Osteochondral alterations in osteoarthritis. *Bone* **51,** 204–211.
64. Wojdasiewicz P, Poniatowski ŁA & Szukiewicz D (2014). The role of inflammatory and anti-inflammatory cytokines in the pathogenesis of osteoarthritis. *Mediators Inflamm* **2014,** 561459.
65. Yamaguchi S, Aoyama T, Ito A, Nagai M, Iijima H, Zhang X, Tajino J & Kuroki H (2013). Effects of exercise level on biomarkers in a rat knee model of osteoarthritis. *Journal of Orthopaedic Research* **31,** 1026–1031.
66. Yeung Tsang K, Wa Tsang S, Chan D & Cheah KSE (2014). The chondrocytic journey in endochondral bone growth and skeletal dysplasia. *Birth Defects Res C Embryo Today* **102,** 52–73.
67. Yoon YM, Oh C Do, Kim DY, Lee YS, Park JW, Huh TL, Kang SS & Chun JS (2000). Epidermal growth factor negatively regulates chondrogenesis of mesenchymal cells by modulating the protein kinase C-α, Erk-1, and p38 MAPK signaling pathways. *Journal of Biological Chemistry* **275,** 12353–12359.
68. Zhen G et al. (2013). Inhibition of TGF-β signaling in mesenchymal stem cells of

subchondral bone attenuates osteoarthritis. *Nat Med* **19,** 704–712.

69. Zhou X, Cao H, Wang M, Zou J & Wu W (2021). Moderate-intensity treadmill running relieves motion-induced post-traumatic osteoarthritis mice by up-regulating the expression of lncRNA H19. *Biomed Eng Online* **20,** 1–22.

Figure legends

Figure 1 Schematic timeline of the experimental protocols. All mice underwent destabilization of the medial meniscus surgery on the right knee and sham surgery on the left knee and then were assigned to either the DMM group (n = 8 mice) or the exercise group (n = 24 mice). The mice in the exercise group were randomly assigned to the DMM + Flat group, DMM + Uphill group, or DMM + Downhill group (n = 8 mice per group). The mice in each exercise group received 3 weeks of treadmill exercise (12 m/min, 30 min/day, and 7 days/week) after exercise habituation. At 4 weeks after DMM induction, the mice were euthanized and evaluated with micro-CT and histological analysis.

Figure 2 3D images of the whole knee joint sample obtained by micro-CT scanning. (**A**) Representative coronal micro-CT images of the total knee joint in mice and sham controls at 4 weeks after DMM induction. (**B**) Changes in bone mineral density (BMD). When compared with the sham group, the BMD increased in all groups (vs DMM group, P = 0.0361; vs DMM + flat group, P = 0.0007; vs DMM + uphill group, P = 0.0007; vs DMM + downhill group, P = 0.0142). (**C**) Changes in bone volume fraction (BV/TV). When

compared with the sham group, the BV/TV increased in all groups (all $P < 0.0001$). When compared with the DMM group, the BV/TV increased in DMM + flat group ($P = 0.0342$) and DMM + uphill group ($P = 0.0271$). Data were presented as mean ± SD. White arrow: bone sclerosis. n = 8 mice per group. Scale bar = 1000 μm.

Figure 3 Histological changes of cartilage in the DMM model after treadmill exercise. (**A**) Safranin O/Fast green staining of cartilage. (**B**) OARSI scores for cartilage structure damage on mice. When compared with the sham group, the OARSI scores increased in all groups (vs DMM group, $P = 0.0030$; vs DMM + flat group, $P = 0.0029$; vs DMM + uphill group, $P = 0.0030$; vs DMM + downhill groups, $P = 0.0031$). When compared with the DMM group, the OARSI scores increased in DMM + flat group ($P = 0.0158$) and DMM + uphill group ($P = 0.0480$). (**C**) Staining intensity of Safranin-O. Data were presented as mean ± SD. white arrow: cartilage damage. n = 8 mice per group. Scale bar = 500 (upper) and 100 (bottom) μm.

Figure 4 Cartilage thickness and chondrocyte density. (**A**) Hematoxylin and eosin staining of cartilage. Uncalcified and calcified layer thickness of cartilage are marked by black solid line. (**B-C**) Thickness and density of the uncalcified and calcified layers of cartilage. Data were presented as mean ± SD. n = 8 mice per group. Scale bar = 500 (upper) and 100 (bottom) μm.

Figure 5 Effects of treadmill exercise on the expression of type II collagen, aggrecan,

and Sox9 of cartilage in the DMM model at 4 weeks postoperatively. (**A**) Immunohistochemistry staining of type II collagen, aggrecan, and Sox9. (**B**) Staining intensity for type II collagen. (**C**) The percentage of aggrecan positive cells. When compared with DMM + flat group, aggrecan-positive chondrocytes increased in both the uncalcified ($P = 0.0065$) and total ($P = 0.0035$) layer cartilage in the DMM + uphill group. (**D**) The percentage of Sox9 positive cells. When compared with the DMM group, Sox9-positive chondrocytes increased in DMM + uphill group (in the uncalcified layer, $P < 0.0001$; in the calcified layer, $P = 0.0005$; in the total layer, $P < 0.0001$) and DMM + downhill group (in the calcified layer, $P = 0.0281$; in the total layer, $P = 0.0253$). When compared to the DMM + flat group, Sox9-positive chondrocytes increased in both the uncalcified ($P = 0.0001$) and total ($P < 0.0001$) layers of cartilage in the DMM + uphill group. When compared with DMM + uphill group, Sox9-positive chondrocytes decrease in both the uncalcified ($P = 0.0006$) and total ($P < 0.0001$) layers of cartilage in the DMM + downhill group. * Significant differences from the DMM group. † Significant differences from the DMM + flat group. ‡ Significant differences from the DMM + uphill group. Data were presented as mean ± SD. n = 8 mice per group. Scale bar = 100 μm.

Figure 6 Effects of treadmill exercise on the expression of MMP-13 and ADAMTS-5 of cartilage in the DMM model at 4 weeks postoperatively. (**A**) immunohistochemistry staining of MMP-13 and ADAMTS-5. (**B**) The percentage of MMP-13 positive cells. When compared with the DMM group, MMP-13-positive chondrocytes decrease in DMM + uphill group (in the calcified layer, $P = 0.0030$; in the total layer, $P = 0.0218$).

When compared with the DMM + flat group, MMP-13-positive chondrocytes decrease in DMM + uphill group (in the calcified layer, $P = 0.0367$). When compared with DMM + uphill group, MMP-13-positive chondrocytes increased in DMM + downhill group (in the total layer, $P = 0.0454$). (**C**) The percentage of ADAMTS-5 positive cells. When compared with the DMM group, ADAMTS-5-positive chondrocytes decrease in DMM + Flat group (in the uncalcified layer, $P = 0.0003$; in the total layer, $P = 0.0001$), DMM + Uphill group (in the uncalcified layer, $P < 0.0001$; in the calcified layer, $P = 0.0090$; in the total layer, $P < 0.0001$), and DMM + downhill group (in the uncalcified layer, $P = 0.0010$; in the total layer, $P = 0.0044$). * Significant differences from the DMM group. † Significant differences from the DMM + flat group. ‡ Significant differences from the DMM + uphill group. Data were presented as mean ± SD. n = 8 mice per group. Scale bar = 100 μm.

Figure 7 Effects of treadmill exercise on the expression of IL-6 and TNF-α of cartilage in the DMM model at 4 weeks *p*ostoperatively. (**A**) immunohistochemistry staining of IL-6 and TNF-α. (**B**) The percentage of IL-6 positive cells. When compared with the DMM group, IL-6-positive chondrocytes decrease in both the DMM + uphill group (in the uncalcified layer, $P = 0.0002$; in the total layer, $P = 0.0002$) and DMM + downhill group (in the uncalcified layer, $P = 0.0285$). When compared with the DMM + flat group, IL-6-positive chondrocytes decrease in DMM + uphill group (in the total layer, *P*

= 0.0436). (**C**) The percentage of TNF-α positive cells. When compared with the DMM group, TNF-α-positive chondrocytes decrease in both the DMM + flat group (in the uncalcified layer, $P = 0.0239$) and DMM + uphill group (in the uncalcified layer, $P = 0.0005$; in the total layer, $P = 0.0105$). When compared with DMM + uphill group, TNF-α-positive chondrocytes increased in DMM + downhill group (in the uncalcified layer, $P = 0.0225$). * Significant differences from the DMM group. † Significant differences from the DMM + flat group. ‡ Significant differences from the DMM + uphill group. Data were presented as mean ± SD. n = 8 mice per group. Scale bar = 100 μm.

Figure

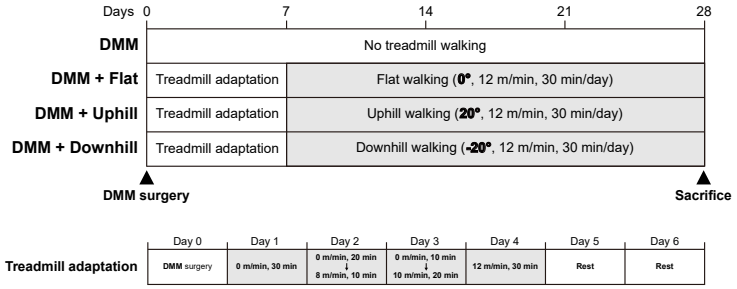
Days 0 7 14 21 28
DMM
No treadmill walking
DMM + Flat
Treadmill adaptation
Flat walking (0°, 12 m/min, 30 min/day)
DMM + Uphill
Treadmill adaptation
Uphill walking (20°, 12 m/min, 30 min/day)
DMM + Downhill
Treadmill adaptation
Downhill walking (-20°, 12 m/min, 30 min/day)
DMM surgery
Sacrifice
Day 0 Day 1 Day 2 Day 3 Day 4 Day 5 Day 6
Treadmill adaptation
DMM surgery
0 m/min, 30 min
0 m/min, 20 min ↓ 8 m/min, 10 min
0 m/min, 10 min ↓ 10 m/min, 20 min
12 m/min, 30 min
Rest
Rest

Fig. 1

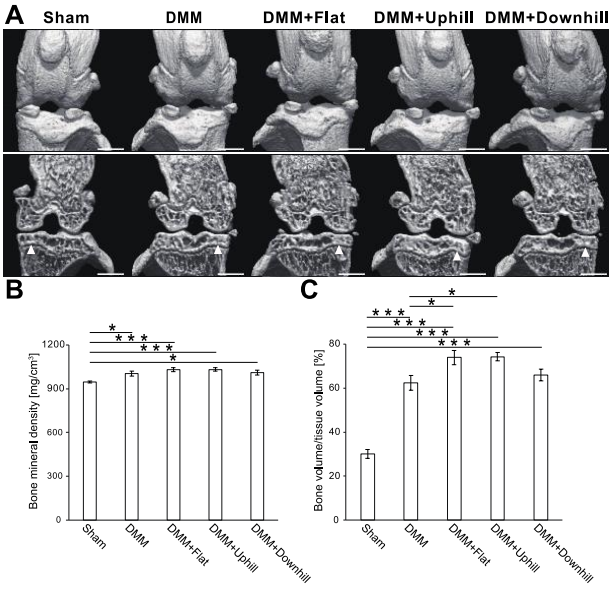
A
Sham
DMM
DMM+Flat
DMM+Uphill
DMM+Downhill
B
Bone mineral density [mg/cm³]
1200
900
600
300
0
Sham
DMM
DMM+Flat
DMM+Uphill
DMM+Downhill
C
Bone volume/tissue volume [%]
80
60
40
20
0
Sham
DMM
DMM+Flat
DMM+Uphill
DMM+Downhill

Fig. 2

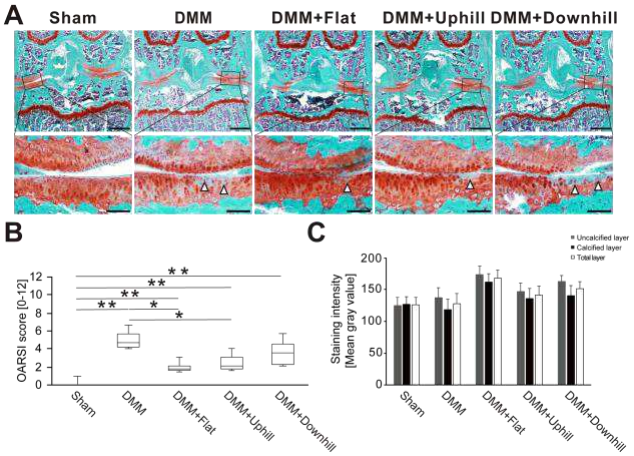
A
Sham
DMM
DMM+Flat
DMM+Uphill
DMM+Downhill
B
OARSI score [0-12]
0
2
4
6
8
10
12
Sham
DMM
DMM+Flat
DMM+Uphill
DMM+Downhill
C
Uncalcified layer
Calcified layer
Total layer
Staining intensity [Mean gray value]
0
50
100
150
200
Sham
DMM
DMM+Flat
DMM+Uphill
DMM+Downhill

Fig. 3

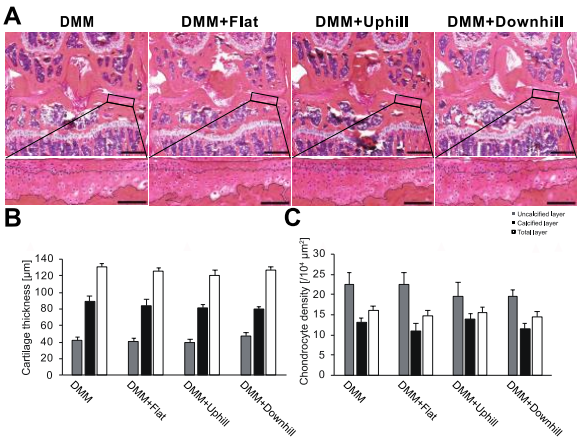
A
DMM
DMM+Flat
DMM+Uphill
DMM+Downhill
B
C
Uncalcified layer
Calcified layer
Total layer
Cartilage thickness [μm]
140
120
100
80
60
40
20
0
DMM
DMM+Flat
DMM+Uphill
DMM+Downhill
Chondrocyte density [/10⁴ μm²]
30
25
20
15
10
5
0
DMM
DMM+Flat
DMM+Uphill
DMM+Downhill

Fig. 4

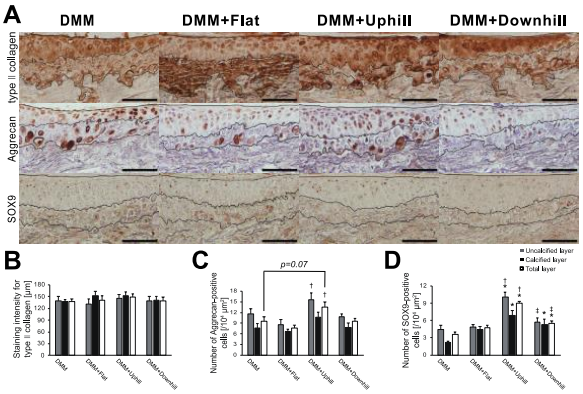
A
DMM
DMM+Flat
DMM+UphiII
DMM+DownhiII
type II collagen
Aggrecan
SOX9
B
C
p=0.07
D
Uncalcified layer
Calcified layer
Total layer

Fig. 5

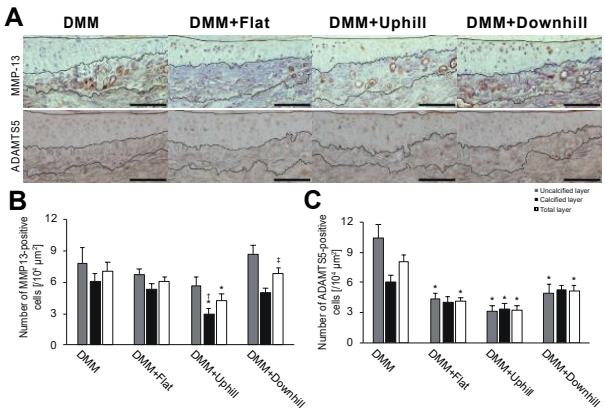
A
DMM
DMM+Flat
DMM+Uphill
DMM+Downhill
MMP-13
ADAMTS5
B
Number of MMP13-positive cells [/10⁴ μm²]
C
Uncalcified layer
Calcified layer
Total layer
Number of ADAMTS5-positive cells [/10⁴ μm²]

Fig. 6

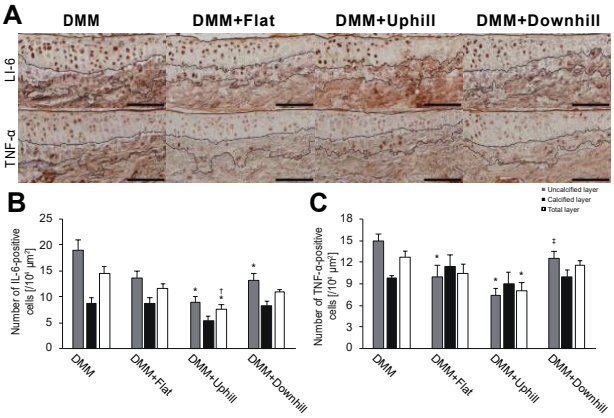
A
DMM
DMM+Flat
DMM+Uphill
DMM+Downhill
LI-6
TNF-α
B
Number of IL-6-positive cells [/10⁴ μm²]
C
Uncalcified layer
Calcified layer
Total layer
Number of TNF-α-positive cells [/10⁴ μm²]
DMM
DMM+Flat
DMM+Uphill
DMM+Downhill

Fig. 7